Fabrication and properties of alginate-hydroxyapatite biocomposites as efficient biomaterials for bone regeneration

Connie Ocando, Sorina Dinescu, Iuliana Samoila, Cristina Daniela Ghitulica, Andreia Cucuruz, Marieta Costache, Luc Avérous

Fabrication and properties of alginate-hydroxyapatite biocomposites as efficient biomaterials for bone regeneration

Connie Ocando[1†], Sorina Dinescu[2], Iuliana Samoila[2], Cristina Daniela Ghitulica [3], Andreia Cucuruz[3], Marieta Costache[2], Luc Avérous[1*]

[1]*BioTeam/ICPEES-ECPM, UMR CNRS 7515, Université de Strasbourg, Strasbourg Cedex 2, France*

[2]*Department of Biochemistry and Molecular Biology, University of Bucharest, 050095, Bucharest, Romania*

[3]*Faculty of Applied Chemistry and Materials Science, University POLITEHNICA of Bucharest 011061 Bucharest, Romania*

***Corresponding author email:** luc.averous@unistra.fr

†Present address: *POLYMAT and Polymer Science and Technology Department, University of the Basque Country (UPV/EHU), Paseo Manuel de Lardizabal 3, Donostia-San Sebastian, 20018, Spain.*

Abstract

Restricted self-recovery that pursues a bone injury and the need of inexpensive and painless clinical treatments for tissue regeneration require new pathways developments to fabricate biocompatible and biodegradable scaffolding materials. For these requirements, covalent crosslinked alginate and alginate/Mg-doped hydroxyapatite (MgHAp) hydrogels are fabricated by “click” chemistry to mimic highly porous structures with the dimensional hierarchy of bone tissue. Cells viability, proliferation and cytotoxicity are reported. These scaffolds show high pore volume with adequate size and interconnectivity for osseous tissue regeneration. An uniform dispersion of low content of bioactive MgHAp nanoparticles on the surface of pore walls allows a good preosteoblast cell attachment and proliferation.

Keywords: alginate, hydroxyapatite, click chemistry, scaffolds, *in vitro* biological behavior.

1. INTRODUCTION

After decades of continuous effort, the research and development on connective tissue engineering [1] for bone regeneration has accomplished remarkable improvement to advance in the replacement of the autograft or allograft treatments that are expensive and painful with high risk of body rejection of transplanted human tissue and infection [2]. Besides, the healing of bone injuries by artificial and not bio-functional tissue scaffolds is still frequently not fully satisfactory. However, numerous biopolymers have demonstrated to be potential alternative strategies in fracture healing and bone regeneration [3].

Thanks to the 3D porous structures of cross-linked hydrogels combined with their water compatibility, these materials are widely used for biomedical purposes, e.g. to simulate tissue regeneration as they can absorb large amounts of biological fluids that allows the diffusion of nutrients to cells. Hydrogels can undergo hydrolytic degradation and finally dissolve or be stable in aqueous media [4]. It has been found that covalently crosslinked hydrogels degrade slower in cell culture medium, which is a key-point for tissue regeneration, compared to more conventional hydrogels based on ionically cross-linked [5]. Nevertheless, covalent cross-linked hydrogels can have a toxic effect on cells, being necessary to find appropriate cell-compatible reagents, or to remove unreacted reagents and by-products.

Alginate is a polysaccharide obtained mostly from brown algae biomass [6, 7]. This biopolymer is a kind of block-copolymer composed of (1-4)-linked β-D-mannuronic acid and α-L-glucuronic acid [8]. In the last decades, alginate-based biomaterials have been extensively applied for biomedical purposes such as drug delivery and tissue engineering due to their biocompatibility, biodegradability, ease gel-forming ability, low toxicity and rather low cost [9, 10, 11]. Biomaterials obtained from purified and alginate develop an suitable environment for osteoblastic differentiation without an inflammatory response in bone forming cells for tissue engineering [12].

In this context, alginate can be crosslinked to forms hydrogels or scaffolds by ionic cross-linking [13, 14, 15], covalent cross-linking [16, 17, 18], thermal gelation [9] or cell cross-linking [19, 20]. Recently and for the first time, a “click”

chemistry approach based on Diels-Alder (DA) reaction was successfully used by our group to crosslink alginate hydrogels. The DA reaction is a [4+2] cycloaddition between a diene and a dienophile that yields a substituted cyclohexene [21-27]. The potential of DA crosslinked alginate hydrogels for drug delivery applications was also clearly demonstrated [27]. However, the cytotoxicity and cell culture of this novel covalent cross-linked hydrogel is still unexplored to develop functional biomaterials for bone regeneration.

On the other hand, hybrid biomaterials combining inorganic fillers and alginate have been largely used to successfully mimic bone tissues [28-35]. In this sense, the bioceramic calcium hydroxyapatite, $Ca_{10}(PO_4)_6(OH)_2$, major inorganic component of bones, has been widely used as a component for tissue regeneration due to its excellent bioactive, osteoconductive and biocompatibility properties that might enhance the rate of bone restoring. Natural hydroxyapatite (HAp) contains various ionic substitutions, such as low concentrations of Mg+2 that plays a vital role in osteoblast proliferation. In this sense, several works has been performed on synthetic Mg based HAp [36]. Cucuruz et al. [37], reported ceramics based on calcium phosphates substituted with Mg^{+2} for bone regeneration. The evaluation of murine preosteoblasts viability and proliferation potential in contact with HAp-Mg biomaterials, a strong positive ratio between live cells and dead cells was found in all composites, suggesting a good biocompatibility of all tested materials. The highest cell density was found in contact with HAp-5wt%Mg.

In the present work, alginate-MgHAp hydrogels were prepared by DA click chemistry to obtain highly porous covalent cross-linked 3D networks . The in vitro biological behaviors of these biomaterials were studied to show their potential as customized biobased templates for tissue engineering purposes. Mg-doped HAp nanoparticles were dispersed into the alginate hydrogel at different compositions and the scaffold adaptiveness to the biological environment as well as the corresponding preosteoblast cellular bioactivity were analyzed.

2. MATERIALS AND METHODS

2.1. Materials

Chemicals and biologicals

Sodium alginate (310-340 kDa) was gently provided by FMC BioPolymer, Ireland (Scheme 1). Poly(propylene oxide)-b-poly(ethylene oxide)-b-poly(propylene oxide) bifunctional maleimide (BMI) with a number-average molar mass of 840 g/mol was obtained from Specific Polymers, France (Scheme 2). Furfurylamine (99%) was obtained from Alfa Aesar. 1-ethyl-3-(3-dimethylaminopropyl) carbodiimide hydrochloride (EDC, Pierce Premium-Grade) was obtained from ThermoFisher Scientific and Phosphate Buffered Saline tablets (PBS) were obtained from Sigma-Aldrich.

Mg oxide nanopowder (<50 nm particles size), Calcium oxide nanopowder (<160 nm particles size determined by BET), phosphoric acid (H_3PO_4 - 85 wt. % in H2O, 99.99% trace metals basis) and ammonium hydroxide solution (NH4OH - ACS reagent, 28.0-30.0% NH3 basis) were purchased by Sigma Aldrich.

Cell proliferation kits, MTT compound and Lactate Dehydrogenase (LDH) assay kits (Tox-7) were purchased from Sigma-Aldrich. LiveDead staining kit was obtained from ThermoFisher Scientific. Cells from MC3T3-E1 cell line and the adequate growth media were purchased from American Type Culture Collection (ATCC).

Synthesis of magnesium-doped hydroxyapatite

Mg-doped HAp (MgHAp) was synthesized. To determine the quantities of raw materials, calculations were performed to obtain HAp with (Ca+Mg)/P ratio of 1.67. The Mg/(Ca+Mg) molar ratio was 0.05. HAp was doped with Mg ions since it has been previously demonstrated that they improve bone cell regeneration [37]. For this purpose, CaO and MgO powders were dispersed in distilled water and homogenized at 300 rpm for 40 min using a Pulverisette 6 planetary ball mill, from Fritsch. Afterwards, 2 M aqueous solution of H_3PO_4 was added dropwise to the suspension at a drip rate of about 0.4 ml/min with a burette with valve. After the completion of this process, the pH was checked and adjusted to around 9.5 by addition of an ammonium hydroxide solution. The precipitate was kept around 24 h at room temperature. The resulting precipitate was then filtered and washed several times with distilled water. Then, it was dried in an oven at 80°C for 24 h. Finally, the powder was thermally treated at 800°C for 2

h at a heating rate of 10°C/min. This thermal treatment was used to calcinate the dry precipitate and to crystallize hydroxyapatite. The temperature of 800 °C was selected from preliminary results obtained from thermal analysis, with TGA. These thermal data suggested the elimination of water and the decomposition of the brushite phase, with the formation of other calcium phosphates which eventually led to the formation of the compound mentioned in the literature [37], The particle size and size distribution examined by SEM has been previously reported in a previous study [37] which reports dimensions range between 100 and 300 nm.

Synthesis of furan-modified alginate

Furan-modified alginate (AF) was obtained by the amidation reaction of the carboxylic groups from the alginate with furfurylamine groups (Scheme 1), following a robust procedure recently reported [27]. Alginate (0.5 g) was dissolved in distilled water (50 mL). Then, the EDC was added to the previous solution in an equimolar ratio with respect to the carboxylic acid groups of the alginate. The solution was continuously stirred during 1 h in order to activate the acid groups. Subsequently, the furfurylamine was added in 1:2 molar ratio with respect to the carboxylic acid groups. The pH was adjusted to around 3.5 through the addition of hydrochloric acid solution. The solution was continuously stirred during 24 h at room temperature. Afterwards, the reactive solution was precipitated in ethanol and the precipitate was washed in distilled water, several times. Finally, the precipitate was dialyzed (Spectra/Por membranes, in 12-14 kDa molar mass cut-off) for 24 h to eliminate unreacted compounds. The corresponding chemically modified compound was then freeze-dried.

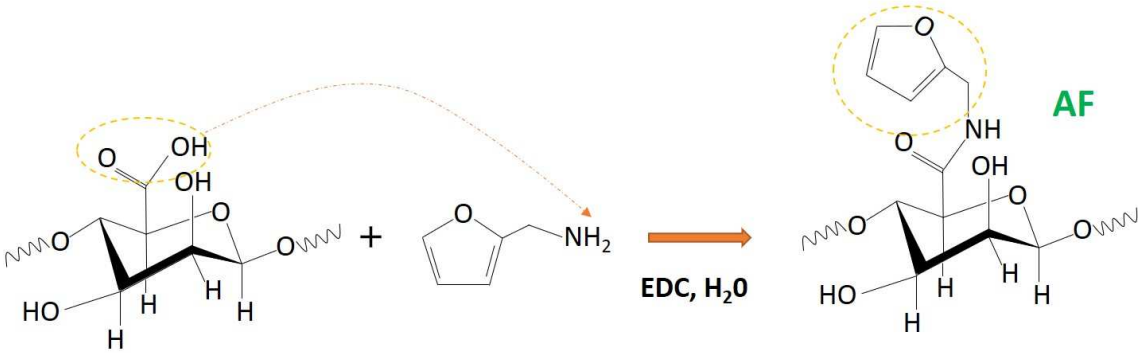

***Scheme 1**. Illustration of the synthesis of AF from alginate by amidation reaction.*

Preparation of DA cross-linked alginate hydrogels and MgHAp biocomposites

Alginate hydrogel was synthetized by cycloaddition reaction between AF (electron-rich diene) and the water-soluble bismaleimide (electron-poor dienophile) to form a furan/maleimide Diels-Alder adduct, responsible of the covalent crosslinking (Scheme 2) [27]. For this purpose, AF (0.1 g) was dissolved in distilled water (1.5 mL). Subsequently, the bismaleimide was added in an equimolar ratio with respect to the furan groups of the AF. Then it was kept at 65 °C during 8 h in a closed container to fully form the alginate hydrogel. Finally, the 3D porous scaffold was freeze-dried.

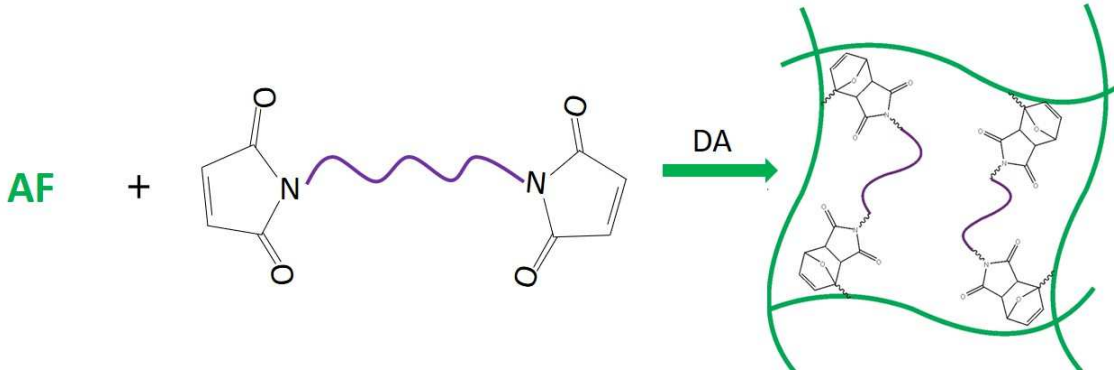

***Scheme 2**. Schematic illustration of the cross-linking between AF and bismaleimide via DA reaction with the genesis of the networks.*

The alginate-MgHAp biocomposites were prepared by addition of different amounts of MgHAp powder (5, 10 and 20 wt.% with respect to alginate). First, the desired amount of MgHAp and distilled water were ultrasonicated for 30 min before adding AF in order to obtain homogeneous MgHAp suspensions without any aggregation. Afterwards, the AF-MgHAp suspension was mixed with the desire amount of bifunctional maleimide and kept at 65 °C during 8 h in a close container to crosslink and form the alginate hydrogel (Figure 1) followed by freeze-drying (Figure 2).

It can be observed that the neat DA cross-linked alginate hydrogel was transparent whereas with the addition of MgHAp the hydrogels become opaque

and white without noticeable macroscopic inhomogeneities (Figure 1). The neat cross-linked alginate hydrogel and their corresponding biocomposites with 5, 10, 20 wt.% of MgHAp are named as HGAF50, HGAF50_5, HGAF50_10, HGAF50_20, respectively.

It is important to emphasize that all hydrogels were immersed in distilled water for 1h to remove possible unreacted compounds before the evaluation of their chemical structure, swelling, hydrolytic degradation, morphological and *in vitro* behavior. ThI cleaning step was repeated 3 times. However, this procedure was not performed to the hydrogels used for the gel content evaluation, in order to estimate their crosslinking degree after the DA click reaction, between AF and bismaleimide.

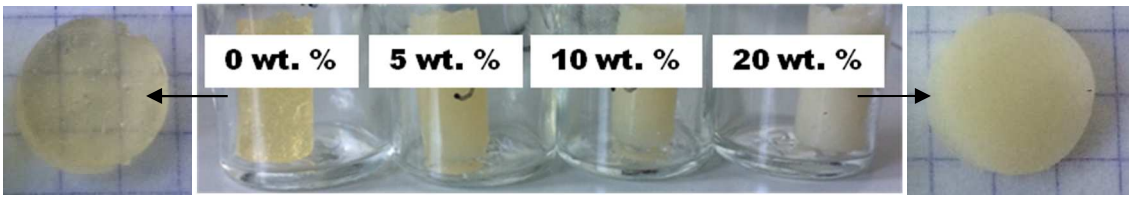

Figure 1. Digital images of neat DA cross-linked alginate and its biocomposites with 5, 10, 20 wt.% of MgHAp after cross-linking via DA reaction.

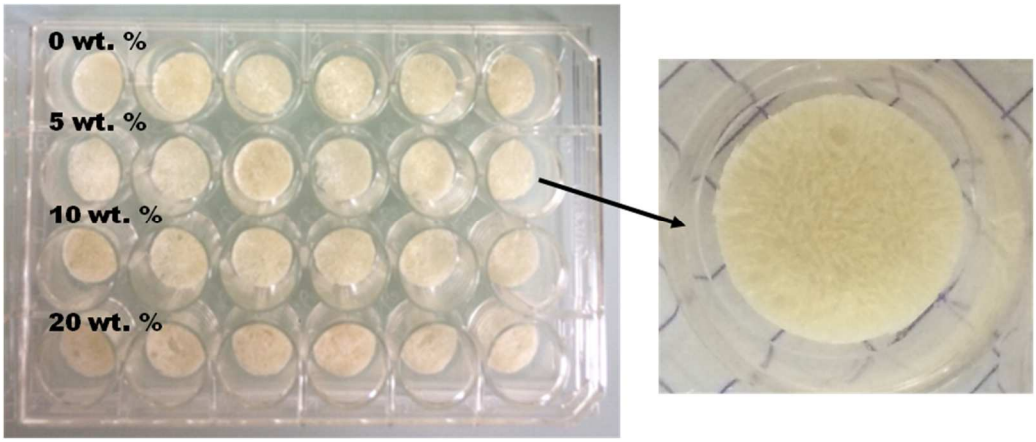

Figure 2. Digital images of neat DA cross-linked alginate and its biocomposites with 5, 10, 20 wt.% of MgHAp after freeze-drying.

2.2. Methods

X-ray diffraction (XRD)

X-ray diffraction analysis was carried out using a Shimadzu XRD 6000 diffractometer at room temperature. It was employed the Cu Kα radiation from a Cu X-ray tube. The sample was scanned in the Bragg angle, 2θ range of 10–80º at a scan rate of 2º/min.

Proton Nuclear Magnetic Resonance (^{1}H NMR)

^{1}H NMR spectra was carried out on a Bruker 500 MHz spectrometer at room temperature in D_2O.

Scanning Electron Microscopy (SEM)

SEM evaluations were carried out using a VEGA3 LM (TESCAN) running at an accelerated voltage of 5 kV. The working distance was around 15 mm. A coating with around 10-20 nm of gold with a sputter coater (QISORS Quorum Technologies) was used. The open source software ImageJ was used to analyze the different images.

Swelling ratio (SR)

The samples were weighed and then immersed in PBS solution at 37 ºC. The swelling ratio was followed during 48 h to obtain an equilibrium. The measurements were carried out in triplicate and an average result was reported. The swelling ratio was evaluated using Equation 1.

$$SR\% = \frac{(W_s - W_d)}{W_d} \times 100 \qquad (1)$$

where W_s is the weight of the swollen and W_d is the weight of freeze–dried hydrogel before swelling ratio evaluation.

Hydrolytic degradation

The samples were weighed and then immersed in PBS solution at 37 ºC to simulate body conditions for 6 days. The samples were removed from the PBS solution and freeze-dried. The measurements were carried out in triplicate and an average result was reported. The hydrolytic degradation was evaluated by calculating the weight loss of the samples using Equation 2:

$$Weight\ Loss\ (\%) = \left({W_0 - W_t}/{W_0}\right) \times 100 \qquad (2)$$

where W_0 and W_t are the freeze-dried weights of the hydrogels before test and after test at each selected time interval, respectively.

In vitro biological behavior

Cell viability and proliferation were evaluated both quantitatively by MTT test and qualitatively by confocal microscopy after staining with calcein acetoxymethyl ester (calceim-AM) and ethidium bromide. Murine preosteoblasts from MC3T3-E1 cell line were seeded on the surface of the porous materials at a density of $2x10^5$ cells/cm^2 and allowed to populate the entire volume of the scaffolds in 24 h, resulting in 3D cultures. Viability test MTT was performed during one week, after 2 and 6 days of culture in standard conditions (37 ˚C, 5% CO_2 and saturated humidity). Briefly, the 3D cultures were incubated in a 1 mg/ml MTT solution and the solution resulting after formazan crystals solubilization in isopropanol was quantified by spectrophotometric measurement at 550 nm. Cytotoxicity assay was carried out using In Vitro Toxicology Assay Kit, Lactic Dehydrogenase-based, following the protocols given by the manufacturer. A 1:1:1 ratio between kit components was used, resulting in a solution that was mixed 2:1 with culture media collected after 2 and 6 days of culture from the samples. The reaction was allowed to develop 20 min in the darkness and then was stopped with 1N HCl. The resulting solution was measured at 490 nm by spectrophotometry. LiveDead assay allowed the qualitative analysis of cell viability and proliferation by differentially staining viable cells in green and dead cells in red. 3D cell cultures were exposed for 1 h to LiveDead solution containing calcein-AM and ethidium bromide homodimer in a proportion recommended by the manufacturer of the kit. Stained cultures were analyzed by confocal microscopy (Zeiss LSM 710, Jena, Germany) and images were processed using Zeiss Zen software.

All experiments were performed in triplicate. Data was analyzed for statistical significance using Graph Pad Prism 6.0 software, One-Way ANOVA method and Bonferroni correction. Statistically significant values were considered for $p<0.05$.

3. RESULTS AND DISCUSSION

3.1. MgHAp characterization

Figure S1 (given in Supporting Information or SI) shows the X-ray diffraction spectrum for 5wt.% Mg-doped HAp. As can be seen, the MgHAp powder showed the characteristic crystalline structure of the main calcium pyrophosphate phase (Ca2P2O7) with a tetragonal structure (a = b = 6.684 Å and c = 24.145 Å). It is possible to emphasize that the presence of Mg phosphate was not identified due to the low Mg concentration, in agreement with reported results [36].

3.2. Characterization of the neat alginate hydrogel and its biocomposites

Furan-modified alginate (AF) was obtained by the amidation reaction of the carboxylic groups from the alginate with furfurylamine groups (Scheme 1). The successfully modification of alginate with furan clickable groups was confirmed by ^{1}H NMR (Figure S2 in SI). The presence of furan protons in AF was confirmed by the appearance of peaks at 6.3, 6.4 and 7.5 ppm [27]. The degree of substitution was calculated by comparing the integrated areas and yield around 50%. This modification will further allow the hydrogel network formation by furan/maleimide DA cross-linking (Scheme 2).

Alginate hydrogel and its biocomposites were developed through click reaction between the furan-modified alginate and the bismaleimide (Figure 1). The gel content in the hydrogels was evaluated in order to confirm the success of the network formation by DA cross-linking. For this purpose, the freeze-dried hydrogel and its biocomposites (Figure 2) were immersed in PBS solution during 1 h. Thus, the unreacted alginate and BMI were dissolved in the PBS solution. Afterwards, the PBS solution containing unreacted compounds was extracted and swollen hydrogels were freeze-dried until not weight changes were detected. The gel content was determined by gravimetric method using the following Equation:

$$GC = \frac{m2}{m1} \times 100 \qquad (3)$$

Where m1 the initial weight of the freeze-dried hydrogel sample and m2 is the weight of the freeze-dried hydrogels after being immersed in PBS.

High gel contents of around 70 w.% were obtained for all the formulations. This gel content value is in perfect agreement with previously reported results for alginate hydrogels with a medium degree of furan substitution [27], meaning that the introduction of MgHAp did not have a negative effect on the crosslinking reaction.

The chemical structure of furan-modified alginate and DA cross-linked alginate and its biocomposite was analyzed by FTIR spectroscopy. To illustrate main results, AF, HGAF50, HGAF50_10 spectra were shown on Figure S3 in SI. The success of the click reaction was also demonstrated by the evolution of the characteristic bands of the carbonyl groups present in the maleimide ring at 1770 and 1697 cm^{-1}. Furthermore, the characteristic band of the C=C bond present in the DA adduct formed at the crosslink point was observed at 1450 cm^{-1}. Besides, the peak for the symmetric stretching (v1) of phosphate is observed at 962 cm^{-1} in the biocomposite.

The microstructure of freeze-dried alginate hydrogel and its biocomposites was analyzed by SEM (Figure 3). Main results are given in Table 1.

Table 1. Morphology of the freeze-dried alginate hydrogel and its biocomposites.

Scaffolds	Pore size (µm)	Pore walls
HGAF50	200-300	Thin and smooth
HGAF50-5	400-500	Thick, rough and with micro- porosities
HGAF50-10	400-700	Thick, rough and with micro- porosities
HGAF50-20	400-700	Thick, highly rough and with micro- porosities

The microstructure of scaffolds used for bone regeneration should present a very specific design factor depending on the seeded cell type and the host osseous tissue to be repaired. Ideally, scaffolds must have an interconnected open pore architecture to ensure the circulation of nutrients and molecules to cells within the scaffold and to the extracellular matrix (ECM) as well as high porosity to ensure cellular proliferation and adhesion. The pores size has to allow cells to migrate and fit inside the scaffold with an adequate large surface area [10]. Even if antagonist results have been published, it has been recently shown that the pore size requirement for an ideal scaffold should be at least 100 µm [4]. As it can be observed on Figure 3, neat alginate scaffold showed a

well-developed pore structure, with a pore size of around 200–300 µm. The surface of the pore walls was quite smooth. Similar results were reported for a hydrogel synthesized from the gelatin, hyaluronic acid and chondroitin sulfate [38]. Moreover, when 5wt.% MgHAp was added, the behavior of the material changes and the pores structure became more complex with bigger pores (400–500 µm) and thicker pore walls with small voids. It has been also found that scaffolds containing multi-scale porosity from micro to macro-scale present enhanced properties when compared with more homogeneous porous scaffolds [39]. With higher MgHAp content (10 and 20 wt.%), a more dense structure was observed with randomly distributed pore size of 400–700 µm combined with small pores around 10-30 µm at the pore walls. SEM images at high magnification of alginate scaffolds modified with MgHAp showed a highly rough surface in the pore walls confirming the impregnation of well-dispersed MgHAp distribution with particle sizes about 10 µm. The surface modification of the pore walls in the scaffold with MgHAp should enhance cells adhesion. In a general way the MgHAp content, modifying the behavior of the material, can tailor a scaffold structure to be adequately adapted to the targeted application.

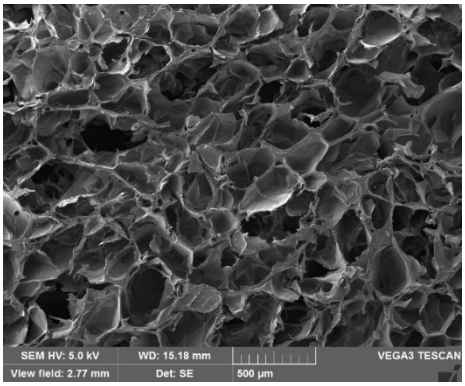

a-i

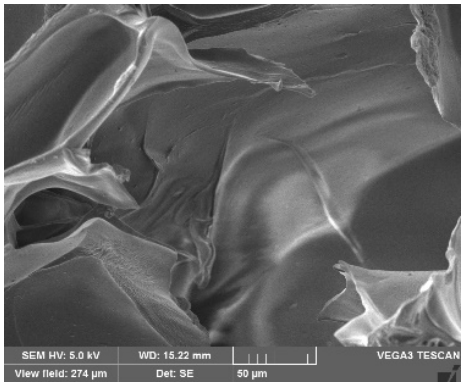

a-ii

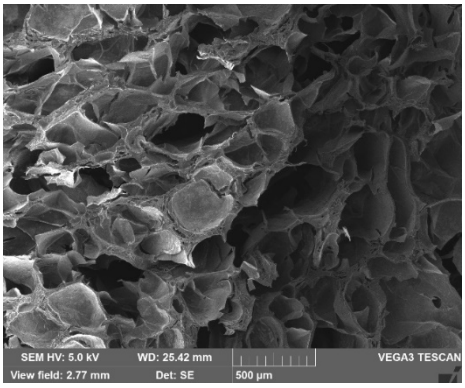

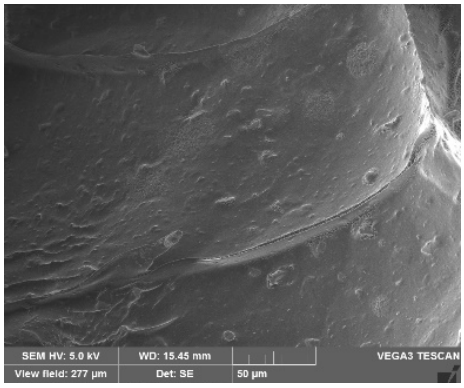

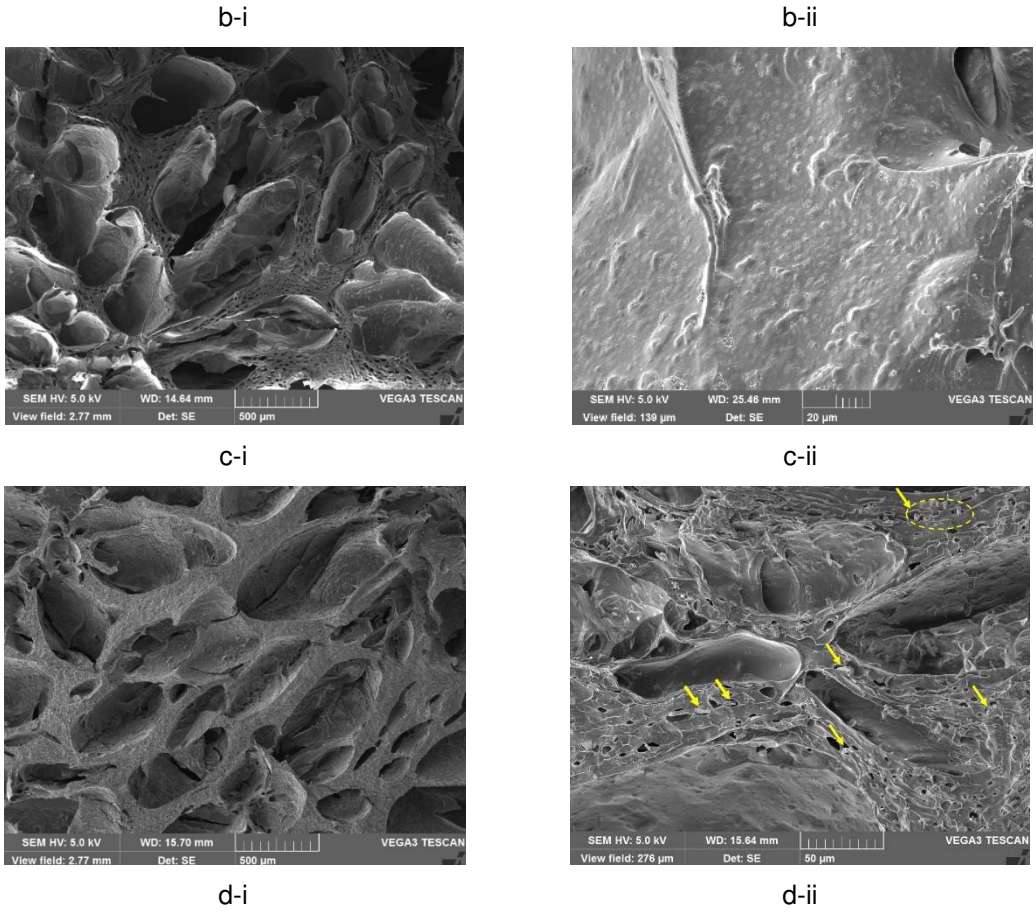

Figure 3. SEM images of the cross-section of freeze-dried hydrogels: a) HGAF50, b) HGAF50_5, c) HGAF50_10 and d) HGAF50_20. Scale bar: i) 500 µm and ii) 50 µm.

The swelling behavior in PBS of freeze-dried alginate hydrogel and biocomposites was determined gravimetrically. The swelling ratio was determined when the equilibrium is reached. All the systems reached the equilibrium after 120 min. The swelling ratio at the equilibrium was 544 ± 10, 545 ± 24, 437 ± 19, 389 ± 8 wt.% for HGAF50, HGAF50_5, HGAF50_10 and HGAF50_20, respectively. In this sense, a decrease in the SR with the increment of MgHAp content is observed. This is in agreement with the morphology of the scaffolds, as HGAF50 and HGAF50_5 with similar porous structured showed similar SR. On the opposite, HGAF50_10 and HGAF50_20 with lower porosity showed lower SR. The hydrolytic degradation in PBS of freeze-dried alginate hydrogel and biocomposites was also investigated by the evaluation of their weight losses as a function of time. After 6 days, the weight loss was 34.3 ± 1.0, 27.9 ± 4.0, 39.9 ± 0.2 and 37.8 ± 3.0 wt.% for HGAF50, HGAF50_5, HGAF50_10 and HGAF50_20, respectively. All the scaffolds

showed values between 28 and 40 wt.% of weight loss. Nevertheless, these differences are not relevant to claim an effect on the hydrolytic degradation with the introduction of MgHAp. The hydrolytic degradation is mainly due to the well-known hydrolysable chemical groups from these macromolecular architectures and materials, such as for instance the amide groups.

3.3. Cell viability and proliferation in contact with alginate hydrogels (neat and biocomposites)

Different complementary biological tests have been performed on these biomaterials. According to MTT assay results, all tested materials registered good levels of biocompatibility, suggesting that the basic composition of modified alginate is adequate for tissue engineering applications. These results are consistent with the ones obtained by Zamani et al. [40], which indicated a high cell viability on alginate-bioactive glass scaffolds. In this study, the alginate-based scaffolds enriched with Zn and Mg were tested in contact with osteoblasts and displayed overall good mechanical and biocompatible properties, as well as antibacterial efficacy. In another study from Sancilio et al. [41], alginate/HAp scaffolds were shown to support efficiently adhesion, colonization and matrix deposition of osteoblast-like cells, therefore providing evidence that the combination of alginate and HAp is biocompatible and osteoconductive. An overall ascending profile of cell proliferation was obtained during one week of culture, with slight differences due to the amount of MgHAp in the composition of the scaffolds (Figure 4). After 2 days of culture, similar levels of viability were found for all biocomposites, with a sensible tendency of increased viability for HGAF50_5 when compared to the control. Viability levels registered for HGAF50_10 and HGAF50_20 remained similar to the ones detected for HGAF50 control material. The tendency observed after 2 days became evident after 6 days of culture, when the highest cell viability was noticed in contact with HGAF50_5, as compared to the control ($p<0.05$). Statistically significant lower viability ($p<0.01$) was registered on HGAF50_10 and HGAF50_20, when compared to HGAF50_5, suggesting that the addition of higher amounts of MgHAp could interfere with cell proliferation rate. Such a behavior has been observed by Mygind et al. [42], as they detected a higher number of viable cells in scaffolds with 500 µm HAp-based porous structure as compared to 200 µm HAp scaffold. In this case, the authors reported fewer but more differentiated mesenchymal stem cells in 200 µm pore-scaffold, while SEM and fluorescence microscopy performed for DNA quantification clearly showed a higher number of cells in 500 µm pore- crystalline structures. Therefore, larger pores encouraged cell viability and proliferation, while smaller pores in HAp materials supported differentiation. In parallel, in our study, the

addition of MgHAp to 10-20% of scaffold structure favored the formation of additional small-sized pores of around 10-30 µm at the pore walls, probably producing a limiting effect on cell proliferation.

Regarding proliferation, the highest statistically significant proliferation ($p<0.001$) was registered on HGAF50_5 after 6 days when compared to 2 days. Similar results were obtained for the control and for HGAF50_10, but to a lower extent ($p<0.01$). However, in the case of cells grown in contact with HGAF50_20, no statistically significant difference was obtained in terms of cell proliferations, suggesting that the addition of 20% MgHAp to HGAF50 composition could limit cell growth.

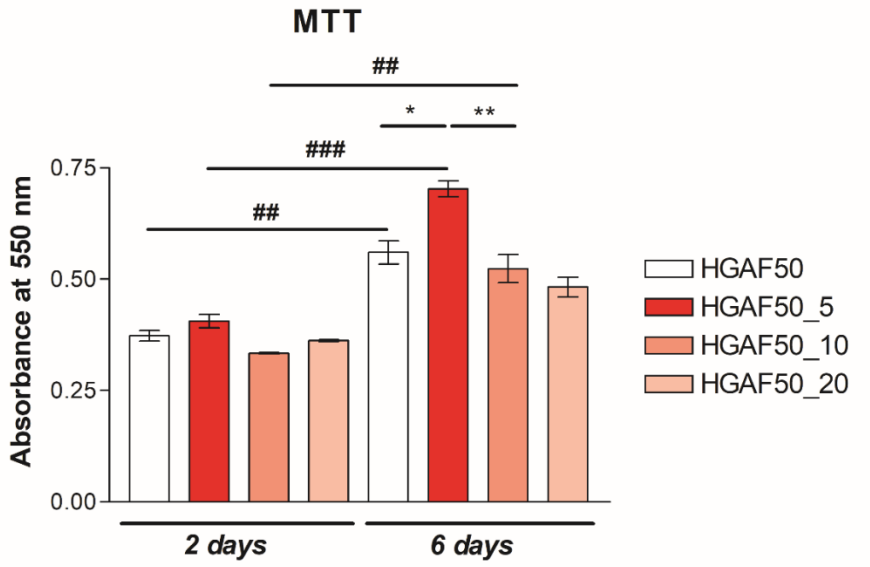

Figure 4. Cell viability and proliferation registered in contact with HGAF50, HGAF50_5, HGAF50_10 and HGAF50_20 after 2 and 6 days of culture, as quantified by MTT assay and spectrophotometry.

3.4. Cytotoxic potential for neat alginate hydrogel and biocomposites

LDH assay was performed to quantify the degree of cytotoxicity exerted by the materials on the cells. Results on Figure 5 showed an overall low cytotoxicity of the materials. Only some cells were found dead, in contact with the biocomposites. Even though small differences between materials cytotoxicity could be observed between 2 and 6 days, none of them were statistically significant. A slight increased cytotoxicity was observed especially on the biocomposites with a higher amount of MgHAp, suggesting that the addition of

higher HAp content could have a detrimental effect for the cells when compared to the control.

LiveDead staining and visualization by confocal microscopy were employed in order to qualitatively observe cell distribution inside the scaffolds and to analyze the ratio between live (green) and dead (red) cells.

Results on Figure 6 support the quantitative results obtained by MTT and LDH assays, showing a high number of viable cells in contact with all biocomposites. Two days after cell seeding, groups of cells were observed on all compositions, especially on HGAF50 and on HGAF50_5 in comparison to HGAF50_10 and HGAF50_20, where smaller cell agglomerations appeared. After 6 days of culture in standard conditions, the greatest number of viable green cells were identified in the with 5% MgHAp in comparison to the control and to the others MgHAp contents. In addition, considerable groups of cells were found in all 3D cultures, supporting the hypothesis that these materials, through their specific structures, could be appropriate for applications in bone regeneration.

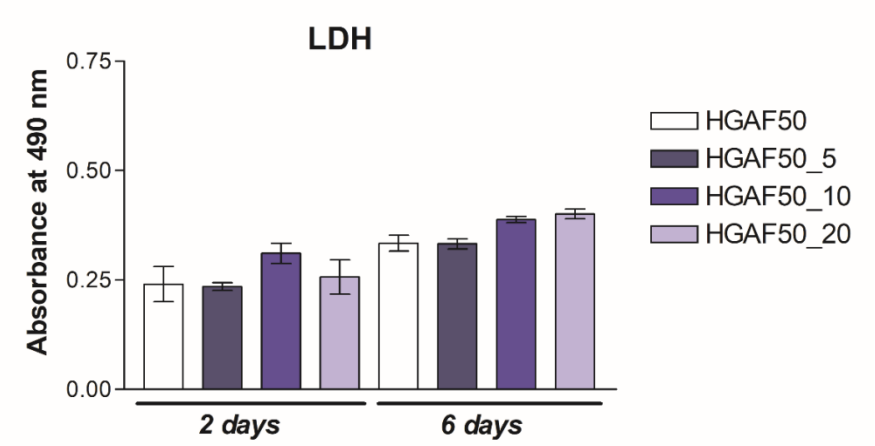

Figure 5. Levels of cytotoxicity registered for HGAF50, HGAF50_5, HGAF50_10 and HGAF50_20after 2 and 6 days of culture, as quantified by LDH assay and spectrophotometry.

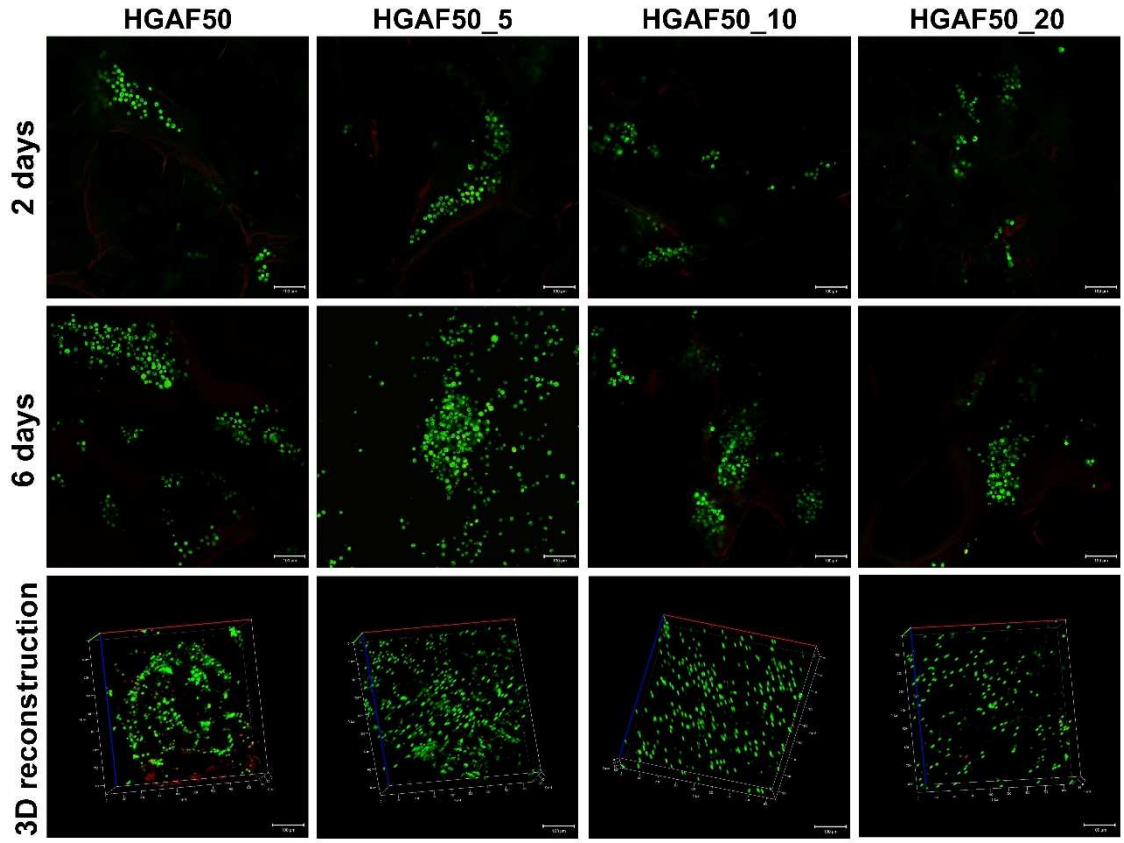

Figure 6. Live (green) and dead (red) cells cultured in contact with HGAF50, HGAF50_5, HGAF50_10 and HGAF50_20after 2 and 6 days of culture, as seen in confocal microscopy; material structure is highlighted in red due to high absorption of the ethidium bromide homodimer fluorescent dye.

4. CONCLUSIONS

Diels–Alder click chemistry is an efficient and non-toxic cross-linking approach to fabricate alginate/hydroxyapatite biocomposite scaffolds with high porosity after freeze-drying. Very specifically, the addition of 5 wt.% MgHAp in the scaffold composition ensures the best development for a biocomposite with a suitable porosity and dimensional hierarchy with good cell–material interactions and excellent cytotoxic properties. The results suggest that the addition of higher amounts of MgHAp in the matrix composition could have a limiting effect on cell behavior. This phenomenon should be investigated in the future to understand better the corresponding mechanisms. In this frame, the effect of the addition of hydroxyapatite must be also studied on the crosslinks of these materials, more particularly at high content.

The biomaterials developed in this work present appropriate microstructure, bioactivity and biocompatibility for uses in bone regeneration because they offer cells a friendly environment for growth and anchoring. Then, the next steps should be also to investigate at the molecular level the cell-substrate interactions and further to test the ability of HGAF50_5 to support cell differentiation towards osteogenic lineage and to evaluate their efficiency on animal models.

Finally, this work constitutes a springboard in the development of biocomposite materials with innovative, biobased and dynamic macromolecular architectures with advanced properties. In the future, the thermo-reversability of the Diels-Alder reaction can be developed to tailor smart and adaptable materials to offer a larger range of biomed applications. In this field, these systems could be developed for instance by 3D or 4D printing.

6. AKNOWLEDGEMENTS

This activity was financed by the National Program III, Subprogram 3.1 Bilateral/Multilateral, Module AUF-RO which are developed in cooperation with the University Agency for Francophony (AUF) with the project BIOCOMPMAT "Composite materials based on biopolymers and ceramic particles with applications in tissue engineering and controlled drug release systems-" 05 AUF and with also the project BIOCOMP3DPRINT "Obtaining composite biomaterials with antibacterial properties by 3D printing technique" (Obtention par impression 3D de biomatériaux composites aux propriétés antibactériennes) - 12 AUF. Another part of this project was funded by East-region in France with MIPPI-4D Project. The biological testing of the materials was supported by a grant of the Romanian Ministry of Research and Innovation, CCCDI- UEFISCDI, project number PNIII-P1-1.2-PCCDI-2017-0782/ 65PCCDI/2018, within PNCDI III.

The authors want to thank Dr. Clara Garcia Astrain (ICPEES, Strasbourg-France) for her advices for the fabrication of the gels, and FMC BioPolymer (Ireland) for providing us the samples of alginate.

Conflict of interest

The authors declare that they have no known competing financial interests or personal relationships that could have appeared to influence the work reported in this paper.

7. REFERENCES

[1] J. J. Li, M. Ebied, J. Xu, H. Zreiqat, Current approaches to bone tissue engineering: the interface between biology and engineering, Adv. Healthcare Mater. 2018, 7, 1701061

[2] S. Bose, M. Roy, A. Bandyopadhyay, Recent advances in bone tissue engineering scaffolds, Trends in biotechnology. 30 (2012), 546-554.

[3] D. M. Gibbs, C. R. Black, J. I. Dawson, R. O. Oreffo, A review of hydrogel use in fracture healing and bone regeneration, J. Tissue Eng. Regen. Med. 10 (2016), 187-198.

[4] E. Caló, V.V. Khutoryanskiy, Biomedical applications of hydrogels: A review of patents and commercial products, Eur. Polym. J. 65 (2015) 252-267.

[5] N. Bhattarai, M. Zhang, Controlled synthesis and structural stability of alginate-based nanofibers, Nanotechnology. 18 (2007) 455601-455611.

[6] C. Gao, E. Pollet, L. Avérous, Innovative plasticized alginate obtained by thermomechanical mixing: Effect of different biobased polyols systems, Carbohydr. Polym. 157 (2017), 669-676.

[7] C. Gao, E. Pollet, L. Avérous, Properties of glycerol-plasticized alginate films obtained by thermo-mechanical mixing, Food Hydrocolloids. 63 (2017), 414-420.

[8] K.I. Draget, C. Taylor, Chemical, physical and biological properties of alginates and their biomedical implications, Food Hydrocolloids. 25 (2011), 251-256.

[9] K.Y. Lee, D.J. Mooney, Alginate: properties and biomedical applications. Prog. Polym. Sci. 37 (2012), 106-126.

[10] F. J. O´Brien, Biomaterials & scaffolds for tissue engineering, Materials today. 14(2011), 88-95.

[11] J. Venkatesan, I. Bhatnagar, P. Manivasagan, K.H. Kang, S.K. Kim, Alginate biocomposites for bone tissue engineering: a review. Int. J. Biol. Macromol. 72 (2015), 269-281.

[12] Torres, M. L., Fernandez, J. M., Dellatorre, F. G., Cortizo, A. M., & Oberti, T. G. (2019). Purification of alginate improves its biocompatibility and eliminates cytotoxicity in matrix for bone tissue engineering. *Algal Research*, *40*, 101499.

[13] C.K. Kuo, P.X. Ma, Ionically crosslinked alginate hydrogels as scaffolds for tissue engineering: Part 1. Structure, gelation rate and mechanical properties, Biomaterials. 22 (2001), 511-521.

[14] A. D. Augst, H.J. Kong, D.J. Mooney, Alginate hydrogels as biomaterials, Macromol. Biosci. 6 (2006), 623-33.

[15] J.L. Drury, R.G. Dennis, D.J. Mooney, The tensile properties of alginate hydrogels, Biomaterials. 25 (2004), 3187-3199.

[16] K.Y. Lee, K.H. Bouhadir, D.J. Mooney, Controlled degradation of hydrogels using multi-functional cross-linking molecules, Biomaterials. 25 (2004), 2461-2466.

[17] K.A. Smeds, M.W. Grinstaff, Photocrosslinkable polysaccharides for in situ hydrogel formation, Journal of Biomedical Materials Research: An Official Journal of The Society for Biomaterials and The Japanese Society for Biomaterials, 54 (2001), 115-121.

[18] R.M. Desai, S.T. Koshy, S.A. Hilderbrand, D.J. Mooney, N.S. Joshi, Versatile click alginate hydrogels crosslinked via tetrazine–norbornene chemistry, Biomaterials. 50 (2015), 30-37.
[19] K.Y. Lee, H.J. Kong, R.G. Larson, D.J. Mooney, Hydrogel formation via cell cross-linking, Adv. Mater. 15 (2003), 1828-1832.
[20] J.L. Drury, T. Boontheekul, D.J. Mooney, Cellular cross-linking of peptide modified hydrogels, J. Biomech. Eng. 127 (2005), 220-228.
[21] A. Gandini, The furan/maleimide Diels–Alder reaction: A versatile click–unclick tool in macromolecular synthesis, Prog. Polym. Sci. 38 (2013), 1-29.
[22] F. Yu, X. Cao, Y. Li, L. Zeng, J. Zhu, G. Wang, X. Chen, Diels–Alder crosslinked HA/PEG hydrogels with high elasticity and fatigue resistance for cell encapsulation and articular cartilage tissue repair, Polym. Chem. 5 (2014), 5116-5123.
[23] C. García-Astrain, I. Algar, A. Gandini, A. Eceiza, M. A. Corcuera, N. Gabilondo, Hydrogel synthesis by aqueous Diels-Alder reaction between furan modified methacrylate and polyetheramine-based bismaleimides, J. Polym. Sci. Part A: Polym. Chem. 53 (2015), 699-708.
[24] C. García-Astrain, A. Gandini, D. Coelho, I. Mondragon, A. Retegi, A. Eceiza, N. Gabilondo, Green chemistry for the synthesis of methacrylate-based hydrogels crosslinked through Diels–Alder reaction. Eur. Polym. J. 49 (2013), 3998-4007.
[25] C. García-Astrain, A. Gandini, C. Peña, I. Algar, A. Eceiza, M. Corcuera, N. Gabilondo, Diels–Alder “click” chemistry for the cross-linking of furfuryl-gelatin-polyetheramine hydrogels. RSC Adv., 4 (2014), 35578-35587.
[26] C. García-Astrain, O. Guaresti, K. González, A. Santamaria-Echart, A. Eceiza, M. A. Corcuera, N. Gabilondo, Click gelatin hydrogels: Characterization and drug release behaviour, Materials letters. 182(2016), 134-137.
[27] C. García-Astrain, L. Avérous, Synthesis and evaluation of functional alginate hydrogels based on click chemistry for drug delivery applications, Carbohydr. Polym. 190 (2018), 271-280.
[28] K. Zhou, X. Zhang, Z. Chen, L. Shi, W. Li, Preparation and characterization of hydroxyapatite–sodium alginate scaffolds by extrusion free forming, Ceram. Int. 41 (2015), 14029-14034.
[29] F. Song, X. Li, Q. Wang, L. Liao, C. Zhang, Nanocomposite hydrogels and their applications in drug delivery and tissue engineering, J. Biomed. Nanotechnol. 11 (2015), 40-52.
[30] K. Sangeetha, A. Thamizhavel, E.K. Girija, Effect of gelatin on the in situ formation of Alginate/Hydroxyapatite nanocomposite, Materials Letters. 91 (2013), 27-30.
[31] Y. Cai, J. Yu, S.C. Kundu, J. Yao, Multifunctional nano-hydroxyapatite and alginate/gelatin based sticky gel biocomposites for potential bone regeneration, Mater. Chem. Phys. 181 (2016), 227-233.
[32] K. Rezwan, Q.Z. Chen, J.J. Blaker, A.R. Boccaccini, Biodegradable and bioactive porous polymer/inorganic biocomposite scaffolds for bone tissue engineering, Biomaterials. 27 (2006), 3413-3431.

[33] M. Swetha, K. Sahithi, A. Moorthi, N. Srinivasan, K. Ramasamy, N. Selvamurugan, Biocomposites containing natural polymers and hydroxyapatite for bone tissue engineering, Int. J. Biol. Macromol. 47 (2010), 1-4.
[34] Y.M. Kolambkar, K.M. Dupont, J.D. Boerckel, N. Huebsch, D.J. Mooney, D.W. Hutmacher, R. E. Guldberg, An alginate-based hybrid system for growth factor delivery in the functional repair of large bone defects, Biomaterials. 32 (2011), 65-74.
[35] Venkatesan, J., Bhatnagar, I., Manivasagan, P., Kang, K. H., & Kim, S. K. (2015). Alginate composites for bone tissue engineering: a review. International journal of biological macromolecules, 72, 269-281.
[36] D. Laurencin, N. Almora-Barrios, N.H. de Leeuw, C. Gervais, C. Bonhommec, F. Mauri, W. Chrzanowski, J.C. Knowles, R.J. Newport, A. Wong, Z. Gan, M.E. Smith, Mg incorporation into hydroxyapatite, Biomaterials. 32 (2011), 1826-1837.
[37] C.D. Ghițulică, A. Cucuruz, G. Voicu, A.T. Cucuruz, S. Dinescu, A. Selaru, M. Costache, Ceramics based on calcium phosphates substituted with Mg ions for bone regeneration, Int. J. App. Ceram. Tech., 17 (2019), 342-353.
[38] F. Yu, X. Cao, L. Zeng, Q. Zhang, X. Chen, An interpenetrating HA/G/CS biomimic hydrogel via Diels–Alder click chemistry for cartilage tissue engineering, Carbohydr. Polym. 97 (2013), 188-195.
[39] J.R. Woodard, A.J. Hilldore, S.K. Lan, C.J. Park, A.W. Morgan, J.A.C. Eurell, S.G. Clark, M.B. Wheeler, R.D. Jamison, A.J.W. Johnson, The mechanical properties and osteoconductivity of hydroxyapatite bone scaffolds with multi-scale porosity, Biomaterials. 28 (2007), 45-54.
[40] D. Zamani, F. Moztarzadeh, D. Bizari, Alginate-bioactive glass containing Zn and Mg biocomposite scaffolds for bone tissue engineering, Int. J. Biol. Macromol. 137 (2019), 1256-1267.
[41] S. Sancilio, M. Gallorini, C. Di Nisio, E. Marsich, R. Di Pietro, H. Schweikl, A. Cataldi, Alginate/Hydroxyapatite-Based Nanocomposite Scaffolds for Bone Tissue Engineering Improve Dental Pulp Biomineralization and Differentiation, Stem Cells International. 2018, 9643721. doi:10.1155/2018/964372.
[42] T. Mygind, M. Stiehler, A. Baatrup, H. Li, X. Zou, A. Flyvbjerg, M. Kassem, C. Bünger, Mesenchymal stem cell ingrowth and differentiation on coralline hydroxyapatite scaffolds, Biomaterials. 28 (2007), 1036-1047.

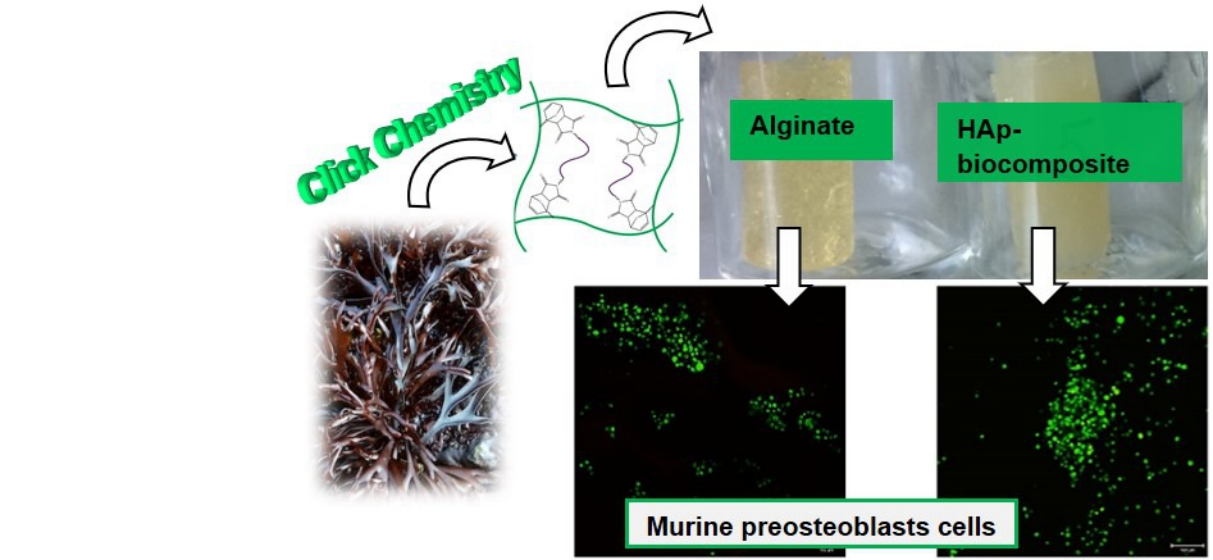
Click Chemistry
Alginate
HAp-
biocomposite
Murine preosteoblasts cells